

where the first term gives the axial potential and the second term gives the nonbonded interactions.

The value of barrier height, 2.8 kcal/mole, obtained thermodynamically, and the value of $V_I(\theta)$ calculated from Eq. (2) give 2.3 kcal/mole for the value of V_0 . On assuming that the intrinsic axial potential is the same for the $\text{CH}_2\text{-CH}_2$ axis of *n*-butane as for the $\text{CH}_3\text{-CH}_3$ axis of ethane, one can calculate the energy to internal rotation for the $\text{CH}_2\text{-CH}_2$ axis of *n*-butane. The whole potential energy of internal rotation for the *n*-butane molecule is given by

$$V = V(\theta_1) + V(\theta_2) + V(\theta_3), \quad (11)$$

where

$$V(\theta_i) = V_0(1 - \cos 3\theta_i) + V_I(\theta_i) \quad (12)$$

and θ_1 , θ_2 , and θ_3 are the angles of internal rotation of

the $\text{CH}_3\text{-CH}_2$, the $\text{CH}_2\text{-CH}_2$, and the $\text{CH}_2\text{-CH}_3$ axes, respectively. The results of calculation are shown in Fig. 11. The energy of the *gauche* form is minimum where θ_1 and θ_3 are 2° and θ_2 is 109° . These values are reasonable as compared with those obtained from the electron diffraction experiments.^{11,12} The calculated energy difference, 1.1 kcal/mole between the *trans* and the *gauche* forms, is somewhat larger than the experimental value, 0.8 kcal/mole.¹³ The agreement is satisfactory, since the attractive potential is not taken into account in Eq. (2) and the attractive term is more important for the energy problems than for the force-constant problems.

¹¹ K. Kuchitsu, J. Chem. Soc. Japan **32**, 748 (1959).

¹² L. S. Bartell and D. A. Kohl, J. Chem. Phys. **39**, 3097 (1963).

¹³ G. J. Szasz, N. Sheppard, and D. H. Rank, J. Chem. Phys. **16**, 704 (1948).

Theoretical Studies of Two-Photon Absorption Processes. I. Molecular Benzene

BARRY HONIG* AND JOSHUA JORTNER

Department of Chemistry, Tel-Aviv University, Tel-Aviv, Israel

AND

ABRAHAM SZÖKE

Department of Physics, Weizmann Institute of Science, Rehovot, Israel

(Received 16 June 1966)

The theory of two-photon transitions is extended to include vibronic-coupling effects. The theory of symmetry-forbidden two-photon transitions is applied for the theoretical study of excitations in benzene. The introduction of vibronic-coupling effects implies that the transition probability should be temperature dependent. A definite assignment of the electronic states of benzene can be obtained from theoretical predictions of the intensity ratios, the vibrational structure, and the polarization dependence for two-photon absorption cross sections in this system.

I. INTRODUCTION

WITH the present availability of intense monochromatic sources of radiation utilizing optical lasers, many types of multipole photon absorption processes in gases,¹⁻³ liquids,⁴ and solids⁵⁻¹² have been

* N.S.F. Predoctoral Fellow, 1964-1966.

¹ J. D. Abella, Phys. Rev. Letters **9**, 453 (1962).

² S. Yatsiv, Phys. Rev. Letters **15**, 614 (1965).

³ J. L. Hall, E. J. Robinson, and L. Branscomb, Phys. Rev. Letters **14**, 1013 (1965).

⁴ J. A. Gordmaine and J. A. Howe, Phys. Rev. Letters **11**, 207 (1963).

⁵ W. Kaiser and C. G. B. Garrett, Phys. Rev. Letters **7**, 229 (1961).

⁶ J. L. Hall, D. A. Jennings and R. M. McClintock, Phys. Rev. Letters **11**, 364 (1963).

⁷ J. J. Hopfield, J. M. Worlock, and K. Park, Phys. Rev. Letters **11**, 414 (1963).

⁸ K. Teegarden, Phys. Rev. **108**, 660 (1957).

⁹ W. L. Peticolas, J. P. Goldsborough, and K. E. Rieckhoff, Phys. Rev. Letters **10**, 93 (1963).

¹⁰ S. Singh and B. P. Stoicheff, J. Chem. Phys. **38**, 2032 (1963).

¹¹ W. L. Peticolas and K. E. Rieckhoff, J. Chem. Phys. **39**, 1347 (1963).

¹² R. G. Kepler, J. C. Caris, P. Avakian and E. Abramson, Phys. Rev. Letters **10**, 400 (1963).

investigated. In intense radiation fields, Maxwell's equations for a dielectric medium are no longer linear, so that the superposition principle is not applicable, and thus waves of different frequencies can interact. From the quantum-mechanical point of view, a non-linear response to an intense optical radiation field can be considered as an interaction leading to mixing of the energy levels of the electronic system by the field, as distinct interactions with weak fields which cause transitions between stationary states. The information obtained from experimental and theoretical studies of two-photon absorption cross sections in atoms, molecules and solids may, in many cases, prove complementary to that obtained from single-photon transitions, in view of the different selection rules for the two processes. In a static system characterized by inversion symmetry, two-photon dipole transitions will take place between states of the same parity. Transitions between such states are dipole forbidden in ordinary single-photon spectroscopy and may be induced only by vibronic-coupling effects. The change

in the selection rules may be readily rationalized by considering the electromagnetic interaction potential for a charged particle, which is given by¹³

$$-(e/mc)(\mathbf{P} \cdot \mathbf{A}) + (e^2/2mc^2)A^2$$

where \mathbf{A} is the vector potential of the radiation field and \mathbf{P} the momentum operator. When the transition probability is expanded in terms of a power series in the electric charge, double-photon transitions, which are determined by the coefficient of e^2 , can take place in first order by means of the A^2 term^{14,15} or in second order by the $(\mathbf{P} \cdot \mathbf{A})$ term.¹⁶ We can confirm that the A^2 term makes only a minor contribution to the transition probability so that the contribution of the absorption of second-harmonic radiation is negligible. On the other hand, the $(\mathbf{P} \cdot \mathbf{A})$ term induces two-photon excitations via intermediate states so that parity is conserved in the electronic transition. In molecules and in solids, these selection rules for two-photon absorption may be relaxed by considering interactions with intramolecular vibrations and with lattice modes, respectively, leading to the admixture of states of opposite symmetry. Vibronic-coupling effects are of major importance in determining the transition probability for symmetry-forbidden two-photon transitions.

It is useful at this stage to summarize the pertinent experimental data regarding two-photon spectroscopy of aromatic molecules. The fluorescence of a number of polycyclic hydrocarbons induced by excitation with a ruby laser ($\hbar\nu = 1.8$ eV) has been reported.^{6,9,10,11,17} The most extensive data are available for crystalline anthracene where fluorescence can be separated into a rapid component which varies with the square of the intensity of exciting light arising from two-photon absorption, and a delayed fluorescence which follows a rather complicated pattern and is due to triplet-triplet annihilation.¹² The mechanism of two-photon absorption in aromatic molecules was clarified by studies of the relative cross sections for one- and two-photon absorption in solution^{11,17} and by the investigations of the polarization of the fluorescence of anthracene induced by two-photon absorption.¹⁸ These experimental data indicate that two-photon excitation in aromatic molecules proceeds via an intermediate virtual state and that the contribution from the A^2 interaction term is negligible. Theoretical calculations have been performed which indicate that this mechanism for two-photon absorption is possible.¹⁹ One should inquire whether symmetry-forbidden two-photon absorp-

tion processes are feasible, and what is the nature of the physical information to be gained from such experiments. Theoretical interpretations of two-photon absorption in anthracene have been contingent upon the presence of either a 1B_g or 1A_g excited state located at 3.6 eV, which is just the double frequency of the laser.^{10,19} Theoretical calculations strongly indicate that these states should be located at higher energies.²⁰ An alternative interpretation is readily available if we assume that a ${}^1A_g \rightarrow {}^1B_{2u}$ two-photon transition takes place. The results presented herein support the hypothesis that a $g \rightarrow u$ vibronically induced two-photon transition takes place via a forbidden pathway, which will still lead to a substantially larger contribution than the absorption of second-harmonic radiation induced by the A^2 term in the interaction Hamiltonian.

In the present paper, we present a theoretical study of a two-photon absorption cross section in benzene arising from $\pi \rightarrow \pi^*$ excitations. The benzene molecule provides a good example illustrating the nature of the additional information available from the studies of two-photon absorption processes. The one-photon ultraviolet absorption spectrum of benzene reveals three bands located at 4.9 ($f = 2 \times 10^{-3}$), 6.2 ($f = 0.1$), and 7.0 eV ($f \sim 1$). The weak band at 4.9 eV and the strong band at 7.0 eV have been assigned to the symmetry-forbidden transition to the ${}^1B_{2u}$ state and to the allowed transition to the ${}^1E_{1u}$ state, respectively.²¹ The 6.2 eV band has been variably assigned to either the ${}^1B_{1u}$ of the ${}^1E_{2g}$ state, but up to date no definite conclusion can be reached on the basis of the vibrational structure²² or from the theoretical analysis of the band intensity or the calculations of the excitation energy.²³ Recent theoretical studies of the benzene molecule^{24,25} using an extensive configuration interaction treatment in the framework of the semiempirical Pariser-Parr-Pople²⁷ scheme yield evidence for the location of the ${}^1E_{2g}$ below the ${}^1B_{1u}$ state. In this work we present a detailed study of the interactions contributing to the two-photon absorption cross sections in this system. The calculations are performed by the Herzberg-Teller²⁸ vibronic-coupling theory. The introduction of vibronic-coupling effects implies that the transition probability should be temperature dependent, and this effect is considered in some detail. Our calculations indicate that a definite assignment of the electronic states of benzene can be obtained from the two-photon absorption spectrum.

¹³ W. Heitler *Quantum Theory of Radiation* (Clarendon Press, Oxford England, 1954), p. 125.

¹⁴ M. Ianuzzi and E. Polacco, *Phys. Rev. Letters* **13**, 371 (1964).

¹⁵ M. Ianuzzi and E. Polacco, *Phys. Rev.* **138**, A806 (1965).

¹⁶ M. Göppert-Mayer, *Ann. Physik* **9**, 273 (1931).

¹⁷ D. H. McMahon, R. A. Soref, and A. R. Franklin, *Phys. Rev. Letters* **14**, 1060 (1965).

¹⁸ W. L. Peticolas and K. E. Rieckhoff, *Phys. Letters* **15**, 230 (1965).

¹⁹ E. M. Evleth and W. L. Peticolas, *J. Chem. Phys.* **41**, 1400 (1964).

²⁰ R. Pariser, *J. Chem. Phys.* **24**, 250 (1956).

²¹ M. Goeppert-Mayer and A. L. Sklar, *J. Chem. Phys.* **6**, 645 (1938).

²² W. E. Donath, *J. Chem. Phys.* **40**, 77 (1964).

²³ F. M. Garforth, C. K. Ingold, and H. G. Poole, *J. Chem. Soc.* **1948**, 555.

²⁴ J. Koutecký, J. Cizek, J. Dubsý, and K. Hlavaty, *Theoret. Chim. Acta* **2**, 462 (1964).

²⁵ J. Koutecký, K. Hlavaty, and P. Hochman, *Theoret. Chim. Acta* **3**, 341 (1965).

²⁶ R. Pariser and R. G. Parr, *J. Chem. Phys.* **21**, 466 (1953).

²⁷ J. A. Pople, *Trans. Faraday Soc.* **49**, 1375 (1953).

²⁸ G. Herzberg and E. Teller, *Z. Physik. Chem.* **B21**, 410 (1933).

II. GENERAL THEORY OF TWO-PHOTON ABSORPTION

We now present an outline of the theory leading to the general expression for the two-photon absorption cross sections as employed in the present work. These results make a direct comparison possible between the contributions of first- and second-order terms in e^2 to the transition probability.

The interaction Hamiltonian between the electronic system and the electromagnetic field is presented in the conventional form

$$H' = -(e/mc) \sum_k \mathbf{p}_k \cdot \mathbf{A}(\mathbf{r}_k) + (e^2/2mc^2) \sum_k [\mathbf{A}(\mathbf{r}_k)]^2, \quad (1)$$

where \mathbf{p}_k and \mathbf{r}_k are the momentum operator (expressed in energy units), and position vector of the k th electron, and \mathbf{A} is the vector potential of the electromagnetic field. The transition probability per unit time from the state 0 to the state F is expressed in the general form

$$\omega_{0F} = \int |K_{0F}|^2 \frac{1 - \cos[(E_F - E_0)t/\hbar] \rho(E_F) dE_F}{(E_F - E_0)^2}. \quad (2)$$

$\rho(E_F)$ is the density of states in the energy interval dE_F , and K_{0F} is the compound two-photon interaction matrix element

$$K_{0F} = \sum_I [H_{0I}^{(1)} H_{IF}^{(1)} / (E_0 - E_I)] + H_{0F}^{(2)}. \quad (3)$$

E_0 , E_I , and E_F are the initial, intermediate, and final energy levels of the composite system consisting of the electromagnetic field and of the electronic system. The summation is taken over all the virtual intermediate states of the composite system. As the intermediate states I are characterized by zero lifetime, energy-conservation rules imply only that $E_0 = E_F$. As usual, the perturbation expansion diverges when $E_0 = E_I$, i.e., when the energy of one photon matches the energy difference between the ground state and an intermediate state of the molecular system. When the system possesses such a channel for direct excitation, the perturbation treatment should be modified to include resonance effects. $H^{(1)}$ and $H^{(2)}$ represent the matrix elements for the interaction terms in the Hamiltonian (1)

$$H_{BC}^{(1)} = -(e/mc) \langle C | \sum_k \mathbf{p}_k \cdot \mathbf{A}(\mathbf{r}_k) | B \rangle,$$

$$H_{BC}^{(2)} = (e^2/2mc^2) \langle C | \sum_k [\mathbf{A}(\mathbf{r}_k)]^2 | B \rangle. \quad (4)$$

Each composite state, say $|B\rangle$, is characterized by an electronic state b and the occupation numbers n_λ of the photon states, so that $|B\rangle = |b, n_1 \dots n_\lambda \dots n_\mu\rangle$. Expanding the vector potential in terms of the creation and annihilation operators of the radiation field and factoring out the field coordinates, the matrix elements (4) take the form

$$H^{(1)}_{b, \dots, n_\lambda \dots | c, \dots, (n_\lambda - 1) \dots} = -(e/mc) (2\pi\hbar^2 c^2 / E_\lambda)^{1/2} (n_\lambda)^{1/2} \langle b | \sum_k \mathbf{p}_k \cdot \mathbf{e}_\lambda \exp i \boldsymbol{\kappa}_\lambda \cdot \mathbf{r}_k | c \rangle, \quad (5a)$$

$$H^{(2)}_{b, \dots, n_\lambda \dots n_\mu \dots | c, \dots, (n_\lambda - 1) \dots (n_\mu - 1) \dots} = (e/2mc^2) (\mathbf{e}_\lambda \cdot \mathbf{e}_\mu) [2\pi\hbar^2 c^2 / (E_\lambda E_\mu)]^{1/2} (n_\lambda n_\mu)^{1/2} \langle b | \sum_k \exp i (\boldsymbol{\kappa}_\lambda + \boldsymbol{\kappa}_\mu) \cdot \mathbf{r}_k | c \rangle, \quad (5b)$$

where E_λ corresponds to the photon energy expressed in terms of the frequency ($E_\lambda = \hbar\omega_\lambda$) or of the angular frequency ($E_\lambda = \hbar\nu_\lambda$), and \mathbf{e}_λ represents the photon wavenumber and its polarization direction, respectively.

The contributions to the matrix elements (3), corresponding to the absorption of the two photons, $\hbar\nu_\lambda + \hbar\nu_\mu$, can be displayed by expanding the exponential terms in Eq. (5) in the form $\exp i \boldsymbol{\kappa} \cdot \mathbf{r}_k = 1 + i \boldsymbol{\kappa} \cdot \mathbf{r}_k$. Furthermore, the energy levels of the composite system are expressed in terms of the electronic energy levels E_0 , E_I and E_F , corresponding to the ground, intermediate and final electronic states, respectively. The compound energy levels are readily expressed in the form $E_0 = E_o + E_\lambda + E_\mu$, $E_I = E_i + E_\lambda$ or $E_I = E_i + E_\mu$, and finally $E_F = E_f$. The second-order interaction term in Eq. (3) can then be displayed in the dipole approximation

$$G = \sum_I \frac{H_{0I}^{(1)} H_{IF}^{(1)}}{E_0 - E_I} = \frac{2\pi e^2 \hbar (n_\lambda n_\mu)^{1/2}}{(E_\lambda E_\mu)^{1/2}} \sum_i (\nu_o \nu_{if}) \times \left[\frac{(\langle 0 | \sum_k \mathbf{r}_k | i \rangle \cdot \mathbf{e}_\lambda) (\langle i | \sum_k \mathbf{r}_k | f \rangle \cdot \mathbf{e}_\mu)}{-\nu_{oi} + \nu_\lambda} + \frac{(\langle 0 | \sum_k \mathbf{r}_k | i \rangle \cdot \mathbf{e}_\mu) (\langle i | \sum_k \mathbf{r}_k | f \rangle \cdot \mathbf{e}_\lambda)}{\nu_{if} - \nu_\lambda} \right], \quad (6)$$

where $\hbar\nu_{oi} = E_i - E_o$ and $\hbar\nu_{if} = E_f - E_i$.

The first-order perturbation matrix element in Eq. (3) arising from the contribution of the A^2 term, can be expressed in the form

$$H^{(2)}_{o, \dots, n_\lambda \dots n_\mu \dots | f, \dots, (n_\lambda - 1) \dots (n_\mu - 1) \dots} = (ie^2/2mc^2) (\mathbf{e}_\lambda \cdot \mathbf{e}_\mu) [2\pi\hbar^2 c^2 / (E_\lambda E_\mu)]^{1/2} (n_\lambda n_\mu)^{1/2} [(\boldsymbol{\kappa}_\lambda + \boldsymbol{\kappa}_\mu) \cdot \langle 0 | \sum_k \mathbf{r}_k | f \rangle]. \quad (7)$$

It is useful at this stage to consider the selection rules for two-photon transitions. One is now faced with the usual difficulties encountered in the use of perturbation expansions, and in some cases we shall be able to proceed with the general analysis only if a smaller number of terms dominate the behavior of the series. From the general form of the matrix elements determining the two-photon transition probability, we conclude that:

(a) For the selection rules for the second-order term large contributions to the sum G arise in the case when the transitions $o \rightarrow i$ and $i \rightarrow f$ are strongly allowed; hence, parity (or inversion symmetry) is expected to be conserved in first order for two-photon transitions when the transition probability is dominated by the second-order perturbation term.

(b) For the selection rules for the first-order term the A^2 interaction term yields a nonvanishing contribution for two-photon absorption corresponding to the same selection rules as for the case of a single-photon absorption.

(c) For the case of polarization dependence the general form of the $H^{(2)}$ interaction matrix element involving the scalar product $(\mathbf{e}_\lambda \cdot \mathbf{e}_\mu)$ implies that in the case of the absorption of two identical circularly polarized photons, $H^{(2)}$ will vanish. This result arises directly from angular-momentum conservation rules. The initial and final compound states are eigenfunctions of angular momentum, since a spin $\pm \hbar$ is assigned to a photon with circular polarization. On the other hand, the contribution from the second-order sum G is, in general, different from zero for circularly polarized radiation. Some experimental work has been reported claiming that double-photon excitation of anthracene by circularly polarized light is characterized by a vanishingly small cross section.¹⁵ However, as we now show, this result is in conflict with general theoretical considerations.

(d) For the relative importance of interactions the ratio of the two contributions G and $H^{(2)}$ to the two-photon excitation cross section can be displayed in the form

$$\rho = (H^{(2)}/G)^2, \quad (8)$$

where we have neglected cross terms arising from interference between the two interactions. The general form of the intensity ratios can be displayed in the form

$$\rho = \left\{ \frac{\hbar(\nu_\lambda + \nu_\mu) r_{of}}{mc \sum_i [\nu_{oi} \nu_{if} r_{oi} r_{if} / (-\nu_{oi} + \nu_\lambda)]} \right\}^2, \quad (9)$$

where $r_{ab} = \langle a | \sum_k \mathbf{r}_k | b \rangle$ and $\nu_{ij} = \nu_j - \nu_i$. If a small number of terms dominate the perturbation expansion, this ratio can be expressed in the approximate form

$$\rho \approx (\hbar/mc r_{oi})^2. \quad (10)$$

Hence, ρ can be expressed in terms of the ratio between the Compton wavelength $\lambda_0 = \hbar/mc$ and a transition moment. Taking a typical transition moment to be of the order $r_{oi} = 0.1-1 \text{ \AA}$, we get $\rho = 10^{-4}-10^{-6}$. Hence, the relative contributions of the A^2 interaction term to the transition probability is expected to be negligible.

(e) For quadrupole two-photon transitions a small contribution to the two-photon transition probability may be due to quadrupole terms arising from the contribution of the second term in the expansion of $\exp(i\mathbf{k} \cdot \mathbf{r})$ to the G sum. The ratio of the quadrupole to the dipole terms is of the order $\eta = [(r_{oi}^2 \kappa_\lambda)/r_{oi}]^2$ so that $\eta \approx (r_{oi}/\lambda)^2$, where λ is the wavelength of the exciting light. Hence, the relative contribution to the transition probability is of the order of $\eta = 10^{-6}$, as in the case of single-photon transitions. The same considerations apply for the case of two-photon magnetic dipole transitions. We thus conclude that the contribution of the quadrupole term is of the same order of magnitude as that corresponding to the A^2 term, and can be safely neglected.

(f) The ratio of single- and double-photon transition probabilities if we assume that only a single intermediate state leads to the dominant contribution to the two-photon transition probability, then the ratio of the cross section for single- and double-photon excitation is given in the form

$$\xi = \left(\frac{2\pi}{\alpha} \right) \frac{r_{if}}{\nu_\lambda} F_\lambda \left[\frac{\nu_{if}}{-\nu_{oi} + \nu_\lambda} \right]^2, \quad (11)$$

where α is the fine-structure constant. Hence, the ratio of single- and double-photon transition probabilities is determined by the intensity of the radiation field. Furthermore, this ratio is inversely proportional to the square of the energy denominator $(-\nu_{oi} + \nu_\lambda)$. This general result indicates that when the energy denominator decreases, but still being larger than the damping factor arising from the natural linewidth, ξ increases quite rapidly. For small values of the energy denominator, one is faced with a quaresonance two-photon absorption effect, first proposed by Yatsiv, which has been applied in case of the potassium laser.² When the energy denominator in Eq. (11) differs appreciably from zero, the bracketed ratio is approximately unity, and the ratio ξ can be expressed by

$$\xi = (2\pi r_{if}^2 / \alpha \nu_\lambda) F_\lambda \approx 10^{-32} F_\lambda. \quad (12)$$

Typical values of F_λ obtained from a giant-pulse ruby laser are $F_\lambda = 10^{28}-10^{30}$ photons/cm²·sec, and thus the ratio of single- and double-photon transition probabilities obtained from (12) is $\xi = 10^{-2}-10^{-4}$.

The arguments presented above lead to a conclusive theoretical evidence that the dominant contribution to the two-photon transition probability arises from the Goeppert-Mayer second-order term G . We now turn our attention to the calculation of the transition prob-

ability for the absorption of a laser photon $\hbar\nu_\lambda$ and another photon $\hbar\nu_\mu$. Utilizing Eqs. (2) and (6) the transition probability per unit is displayed in the form

$$\omega_{0F} = (8\pi^2 e^4 / \hbar^4 c^2) [F_\lambda \hbar\nu_\lambda I_\mu |M|^2 / (\nu_\lambda \nu_\mu)^2], \quad (13)$$

where $I_\mu d\nu_\mu$ is the intensity of one light beam (expressed in units of energy per square centimeter·second) and $F_\lambda = I_\lambda d\nu_\lambda / E_\lambda$ is the flux of the laser beam, while the interaction matrix element is given in the form

$$M = \sum_i (\nu_{oi} \nu_{if}) \left[\frac{(\mathbf{r}_{oi} \cdot \mathbf{e}_\lambda)(\mathbf{r}_{if} \cdot \mathbf{e}_\mu)}{-\nu_{oi} + \nu_\lambda} + \frac{(\mathbf{r}_{oi} \cdot \mathbf{e}_\mu)(\mathbf{r}_{if} \cdot \mathbf{e}_\lambda)}{\nu_{if} - \nu_\lambda} \right]. \quad (14)$$

[*Note added in proof:* The application of momentum-coordinate commutation relations leads to the expression

$$M = \nu_\lambda \nu_\mu \sum_i \left[\frac{(\mathbf{r}_{oi} \cdot \mathbf{e}_\lambda)(\mathbf{r}_{if} \cdot \mathbf{e}_\mu)}{-\nu_{oi} + \nu_\lambda} + \frac{(\mathbf{r}_{oi} \cdot \mathbf{e}_\mu)(\mathbf{r}_{if} \cdot \mathbf{e}_\lambda)}{\nu_{if} - \nu_\lambda} \right]. \quad (14a)$$

Equation (14a) is expected to lead to a better conversion of the perturbation series.]

The total transition probability ω_{0F} can now be expressed in terms of the transition probability per unit time per unit frequency, and a line-shape function $g(\nu_\mu)$, so that

$$\omega(\nu_\mu) = \omega_{0F} g(\nu_\mu) d\nu_\mu \quad (15)$$

and

$$\int g(\nu_\mu) d\nu_\mu = 1. \quad (16)$$

The cross section for two-photon absorption per unit of angular frequency is given by

$$\sigma(\nu_\mu) = \hbar \nu_\mu \omega(\nu_\mu) / I_\mu \quad (17)$$

so that

$$\sigma(\nu_\mu) = \frac{8\pi^2 e^4 g(\nu_\mu) F_\lambda |M|^2}{\hbar^2 c^2 (\nu_\lambda \nu_\mu)}. \quad (18)$$

Finally, it is convenient to display the cross section for two-photon absorption per unit frequency ($\omega_\mu = \nu_\mu / 2\pi$):

$$\begin{aligned} \sigma(\omega_\mu) &= \frac{4\pi^2 e^4 g(\omega_\mu) F_\lambda}{\hbar^2 c^2 (\omega_\lambda \omega_\mu)} \\ &\times \left\{ \sum_i (\omega_{oi} \omega_{if}) \left[\frac{(\mathbf{r}_{oi} \cdot \mathbf{e}_\lambda)(\mathbf{r}_{if} \cdot \mathbf{e}_\mu)}{-\omega_{oi} + \omega_\lambda} + \frac{(\mathbf{r}_{oi} \cdot \mathbf{e}_\mu)(\mathbf{r}_{if} \cdot \mathbf{e}_\lambda)}{\omega_{if} - \omega_\lambda} \right] \right\}^2. \end{aligned} \quad (19)$$

III. VIBRONIC COUPLING IN TWO-PHOTON TRANSITIONS

A. Vibronic Coupling

Application of group theoretical considerations to the Goeppert-Mayer sums determines the symmetry

of the final state in a two-photon transition. However, as in the case of one-photon excitations, the possibility of symmetry-forbidden two-photon transitions must be considered. The principal cause of intensity in spin-allowed, symmetry-forbidden one-photon transitions arises from vibronic coupling between electronic states.²⁸⁻³¹ Since the two-photon transition probabilities are determined by the products of transition dipoles, it is expected that the effects of vibronic coupling should be similar for the cases of one- and two-photon transitions.

The vibronic wavefunction of a molecule is expressed in the Born-Oppenheimer approximation as a product of an electronic wavefunction $\Theta_k(x, q)$ and a vibrational function $\Phi_{kj}(q)$:

$$\Psi_{kj}(x, q) = \Theta_k(x, q) \Phi_{kj}(q), \quad (20)$$

where x and q refer to a complete set of electronic and nuclear coordinates, k is an electronic state for fixed q , and j is a vibrational state. The transition probability between the vibronic states gi and kj is determined by the square of the absolute value of the transition moment.

$$M_{gi,kj} = \int \Phi_{gi}^*(q) M_{gk}(q) \Phi_{kj}(q) dq, \quad (21)$$

where

$$M_{gk}(q) = \int \Theta_g^*(x, q) \mathbf{m}_e(x) \Theta_k(x, q) dx. \quad (22)$$

$\mathbf{m}_e(x)$ represents the electronic-transition dipole operator. In the Herzberg-Teller theory, the electronic wavefunction is expanded in terms of the wavefunctions corresponding to zero nuclear displacement:

$$\Theta_k(x, q) = \Theta_k^0(x, 0) + \sum_s \lambda_{ks}(q) \Theta_s^0(x, 0), \quad (23)$$

where the mixing coefficient λ_{ks} is

$$\lambda_{ks}(q) = \frac{1}{E_s - E_k} \int \Theta_k^0(x, 0) H^1(q) \Theta_s^0(x, 0) dx. \quad (24)$$

$\Theta_k^0(x, 0)$ is the ground-state electronic wavefunction for the molecule in its equilibrium nuclear configuration, $H^1(q)$ is the perturbation Hamiltonian arising from nuclear displacements.

The perturbation potential $H^1(q)$ may be derived by expanding the Hamiltonian in powers of the set of the normal coordinates q_a :

$$H^1(q) = \sum_a H^1(q_a), \quad (25)$$

where

$$H^1(q_a) = q_a (\partial H / \partial q_a)_0. \quad (26)$$

²⁹ J. N. Murrell and J. A. Pople, Proc. Phys. Soc. (London) **A69**, 245 (1956).

³⁰ A. C. Albrecht, J. Chem. Phys. **33**, 156, 169 (1960).

³¹ A. D. Liehr, Can. J. Phys. **35**, 1123 (1957); **36**, 1588 (1957).

The only term in the electronic Hamiltonian depending on nuclear coordinates involves the electron-nuclear Coulomb interactions

$$H'(q_a) = -q_a (\partial/\partial q_a) \sum_i \sum_\sigma (\partial H_{i\sigma}/\partial \mathbf{r}_\sigma)_0 (\partial \mathbf{r}_\sigma/\partial q_a)_0, \quad (27)$$

where

$$H_{i\sigma} = Z_\sigma e^2 / r_{i\sigma}. \quad (28)$$

In Eqs. (27) and (28) Z represents the nuclear charges, \mathbf{r}_σ are the nuclear coordinates, $\mathbf{r}_{i\sigma}$ the electron-nucleus position vectors, and the derivatives $(\partial \mathbf{r}_\sigma/\partial q_a)_0$ correspond to the elements of the matrix which transforms from the normal coordinates q_a to the Cartesian displacement coordinates in the ground state.

The general expression for the mixing coefficients becomes

$$\lambda_{ks}(q) = [1/(E_s - E_k)] \sum_a q_a (W_{ks})_a, \quad (29)$$

where

$$(W_{ks})_a = \sum_\sigma \int \rho_{ks}(p) Z_\sigma e^2 \left(\frac{\partial \mathbf{r}_\sigma}{\partial q_a} \right)_0 \frac{\mathbf{r}_{i\sigma}}{r_{i\sigma}^3} dx_p \quad (30)$$

and

$$\rho_{ks}(p) = n \int \Theta_s^0(x, 0) \Theta_k^0(x, 0) dx^1 \quad (31)$$

represents the one-electron transition density (or the rearrangement density) of the n -electron system. The integration in Eq. (30) is taken over $n-1$ electronic coordinates, excluding the coordinates of the p th electron. We now invoke the usual assumption that the ground-state mixing is negligible in view of the relatively large energy denominators arising in Eq. (23). Introducing Eq. (23) into Eq. (22), we obtain

$$M_{gk}(q) = M_{gk}^0 + \sum_s \lambda_{ks}(q) M_{gs}^0. \quad (32)$$

For a symmetry-forbidden transition $M_{gk}^0 = 0$.

The condition for the appearance of a symmetry-“forbidden” band is that for some s , both M_{gs}^0 and $\lambda_{ks}(q)$ will be nonvanishing. Thus, M_{gs}^0 must correspond to some spin- and symmetry-allowed electronic transition. In order that $\lambda_{ks}(q)$ not vanish, the integrand in Eq. (24) must form the basis for a totally symmetric representation. This requirement essentially specifies the symmetry of the vibrations participating in the vibronic coupling. The transition moment (21) for the case of a symmetry-forbidden transition between the vibronic states gi and kj can now be displayed in the form

$$M_{gi,kj} = \sum_s [M_{gs}^0 / (E_s - E_k)] \sum_a (W_{ks})_a \langle \Phi_{gi} | q_a | \Phi_{kj} \rangle. \quad (33)$$

It is useful at this stage to consider the total transition probability P_{gk} for the electronic transition $g \rightarrow k$. Application of an approximate quantum-mechanical

sum rule leads to the result

$$P_{gk} = \sum_i B_i \langle \Phi_{gi} | M_{gk}^2 | \Phi_{gi} \rangle, \quad (34)$$

where B_i is the Boltzman weighting factor for the level gi . The matrix element (33) can be displayed in the form

$$\langle M_{gk}^2 \rangle_{ii} = \sum_a \sum_s \frac{M_{gs}^0}{E_s - E_k} \times \int \rho_{sk}(P) \sum_\sigma Z_\sigma e^2 \left(\frac{\partial \mathbf{r}_\sigma}{\partial q_a} \right)_0 \langle q_a^2 \rangle_{ii} \frac{\mathbf{r}_{i\sigma}}{r_{i\sigma}^3} dx_p, \quad (35)$$

where $\langle q_a^2 \rangle_{ii}$ is the root-square displacement of the normal coordinate of the a th normal mode in the i th vibrational state of the ground electronic state. In the harmonic-oscillator approximation, $\langle q_a^2 \rangle_{ii}$ is found to be $(\nu_i + \frac{1}{2})(\hbar/4\pi^2\omega_a)$, where ω_a is the characteristic frequency of the a th mode.

Finally, the transition probability for a one-photon transition can be displayed in the form

$$P_{gk} = \sum_a \sum_s [M_{gs}^0 / (E_s - E_k)] \times [(W_{ks})_a \langle q_a^2 \rangle_{00}]^2 \coth(\hbar\omega_a/2kT). \quad (36)$$

The temperature dependence of the transition probability arises from the $\langle q_a^2 \rangle_{ii}$ terms in Eq. (35).

The integrals arising from Eq. (35) have been evaluated by both semiempirical²⁹ and more rigorous methods.³¹ Useful simplifications arising from symmetry considerations have been introduced by Albrecht.³⁰ In the present work, we employ both Murrell-Pople semiempirical method and the Liehr³¹-Albrecht³⁰ non-empirical scheme. In the Murrell-Pople method, the perturbation energy is approximated by the introduction of the one-electron transition density $\rho_{sk}(p)$ and the set of dipoles representing the nuclear displacements in the various normal modes. The integral in Eq. (35) is then represented by the classical interaction energy of the set of dipoles $Z_\sigma e^2 (\partial \mathbf{r}_\sigma/\partial q_a)_0$ and the transition density $e\rho_{sk}(p)$.

B. Symmetry-Forbidden Two-Photon Transitions

The two-photon transition probability between the vibronic states gi and fj is proportional to the square of the Goeppert-Mayer sum:

$$S_{gi,fj} = \sum_{kl} \Gamma_{gi,fj}^{kl} [(M_{gi,kl}^\lambda M_{kl,fj}^\mu / \Delta_{gi,kl}^\lambda) + (M_{gi,kl}^\mu M_{kl,fj}^\lambda / \Delta_{gi,kl}^\mu)], \quad (37)$$

where

$$M_{gi,kl}^\lambda = (\mathbf{M}_{gi,kl} \cdot \mathbf{e}_\lambda), \quad (38)$$

$$\Delta_{gi,kl}^\lambda = -\nu_{gi,kl} + \nu_\lambda, \quad (39)$$

and

$$\Gamma_{gi,fj}^{kl} = \nu_{gi,k} \nu_{kl,fj} / \nu_\lambda \nu_\mu. \quad (40)$$

Excluding the case of resonance effects, it is possible without serious error to replace $\Delta_{gi,kl}^\lambda$ and $\Gamma_{gi,fj}^{kl}$ by

their electronic mean values $\Delta_{g,k}^\lambda$ and $\Gamma_{g,f}^k$. For a symmetry-allowed two-photon transition, the transition moment is proportional to

$$K_{gi,fj} = |S_{gi,fj}|^2 = \left| \sum_{kl} \Gamma_{g,f}^k [(M_{g,k}^{0,\lambda} M_{k,f}^{0,\mu} \langle gi | kl \rangle \langle kl | fj \rangle / \Delta_{g,k}^\lambda) + (M_{g,k}^{0,\mu} M_{k,f}^{0,\lambda} \langle gi | kl \rangle \langle kl | fj \rangle / \Delta_{g,k}^\mu)] \right|^2, \quad (41)$$

where we have introduced

$$M_{gi,kl}^\lambda = M_{g,k}^{0,\lambda} \langle gi | kl \rangle \quad (42)$$

and a simplified notation is applied for the integration over nuclear coordinates. The total transition probability for a two-photon absorption process is displayed in the form

$$P_{g,f} = \sum_i B_i \sum_j K_{gi,fj}. \quad (43)$$

Application of the quantum-mechanical sum rules

$$\begin{aligned} \sum_i \langle gi | kl \rangle \langle kl | fj \rangle &= \langle gi | fj \rangle, \\ \sum_i B_i \sum_j |\langle gi | fj \rangle|^2 &= 1, \end{aligned} \quad (44)$$

lead to the result

$$P_{g,f} = \left| \sum_k \Gamma_{g,f}^k [(M_{g,k}^{0,\lambda} M_{k,f}^{0,\mu} / \Delta_{g,k}^\lambda) + (M_{g,k}^{0,\mu} M_{k,f}^{0,\lambda} / \Delta_{g,k}^\mu)] \right|^2. \quad (45)$$

Thus, symmetry-allowed two-photon transitions exhibit no temperature dependence of the transition probability, as might be expected.

We now turn our attention to the case of two-photon symmetry forbidden transitions. In general, the transition moments can be expanded in a Taylor series of nuclear displacements:

$$M_{gi,kl} = M_{g,k}^{0,\lambda} \langle gi | kl \rangle + \sum_s M_{gs}^{0,\lambda} (E_s - E_k)^{-1} \sum_a (W_{ks})_a \langle gi | q_a | kl \rangle + \sum_{s'} M_{ks'}^{0,\lambda} (E_{s'} - E_g)^{-1} \sum_a (W_{gs'})_a \langle gi | q_a | kl \rangle. \quad (46a)$$

In a similar way, we write

$$M_{kl,fj} = M_{k,f}^{0,\lambda} \langle kl | fj \rangle + \sum_p M_{kp}^{0,\lambda} (E_p - E_f)^{-1} \sum_a (W_{fp})_a \langle kl | q_a | fj \rangle + \sum_{p'} M_{f,p'}^{0,\lambda} (E_p - E_k)^{-1} \sum_a (W_{kp'})_a \langle kl | q_a | fj \rangle. \quad (46b)$$

The inclusion of the second sum in Eq. (46a) is equivalent to the introduction of ground-state vibronic coupling in the case of one-photon symmetry-forbidden transitions. The inclusion of the second sum on the right-hand side of Eq. (46b) is necessary in view of the importance of vibronic coupling between the intermediate state and other excited states.

The matrix elements (37) can now be represented to the first order in q_a in the form

$$S_{gi,fj} = \alpha \sum_i \langle gi | kl \rangle \langle kl | fj \rangle + \sum_i \sum_a \beta_a \langle kl | q_a | fj \rangle \langle gi | kl \rangle + \sum_i \sum_a \gamma_a \langle gi | q_a | kl \rangle \langle kl | fj \rangle, \quad (47)$$

where

$$\alpha = \sum_k \Gamma_{g,f}^k [(M_{g,k}^{0,\lambda} M_{k,f}^{0,\mu} / \Delta_{g,k}^\lambda) + (M_{g,k}^{0,\mu} M_{k,f}^{0,\lambda} / \Delta_{g,k}^\mu)], \quad (48)$$

$$\begin{aligned} \beta_a = \sum_k \Gamma_{g,f}^k \left[\sum_p \left(\frac{M_{g,k}^{0,\lambda} M_{k,p}^{0,\mu}}{\Delta_{g,k}^\lambda} + \frac{M_{g,k}^{0,\mu} M_{kp}^{0,\lambda}}{\Delta_{g,k}^\mu} \right) (E_p - E_f)^{-1} (W_{fp})_a + \right. \\ \left. + \left(\frac{M_{g,k}^{0,\lambda} M_{f,p}^{0,\mu}}{\Delta_{g,k}^\lambda} + \frac{M_{g,k}^{0,\mu} M_{f,p}^{0,\lambda}}{\Delta_{g,k}^\mu} \right) (E_p - E_k)^{-1} (W_{kp})_a \right], \end{aligned} \quad (49)$$

and

$$\begin{aligned} \gamma_a = \sum_k \Gamma_{g,f}^k \left[\sum_s \left(\frac{M_{g,s}^{0,\lambda} M_{k,f}^{0,\mu}}{\Delta_{g,k}^\lambda} + \frac{M_{g,s}^{0,\mu} M_{kf}^{0,\lambda}}{\Delta_{g,k}^\mu} \right) (E_s - E_k)^{-1} (W_{ks})_a \right. \\ \left. + \left(\frac{M_{k,s}^{0,\lambda} M_{k,f}^{0,\mu}}{\Delta_{g,k}^\lambda} + \frac{M_{k,s}^{0,\mu} M_{k,f}^{0,\lambda}}{\Delta_{g,k}^\mu} \right) (E_s - E_g)^{-1} (W_{gs})_a \right]. \end{aligned} \quad (50)$$

The appropriate quantum-mechanical sum rules are now introduced to give

$$\begin{aligned}\sum_i \langle gi | q_a | kl \rangle \langle kl | fj \rangle &= \langle gi | q_a | fj \rangle, \\ \sum_i \langle gi | kl \rangle \langle kl | q_a | fj \rangle &= \langle gi | q_a | fj \rangle.\end{aligned}\quad (51)$$

The Goeppert-Mayer sum can now be presented in the form

$$S_{gi,fj} = \alpha \langle gi | fj \rangle + \sum_a \delta_a \langle gi | q_a | fj \rangle, \quad (52)$$

where

$$\delta_a = \beta_a + \gamma_a. \quad (53)$$

For the case of a symmetry-forbidden two-photon transition when either $M_{g,k}^0$ or $M_{k,f}^0$ vanishes, we obtain the result

$$S_{gi,fj} = \sum_a \delta_a \langle gi | q_a | fj \rangle. \quad (52')$$

The total transition probability is then given by

$$P_{g,f} = \sum_i B_i \sum_j \left(\sum_a \delta_a \langle gi | q_a | fj \rangle \right)^2. \quad (43')$$

Invoking the sum rule again, we obtain

$$P_{g,f} = \sum_a \delta_a^2 \langle gi | q_a^2 | gi \rangle \coth(\hbar\omega_a/2kT). \quad (54)$$

A discussion of the selection rules for symmetry-forbidden two-photon transitions is of interest. Implicit in what follows, practical validity is assumed of the Herzberg-Teller expansion and of the approximate quantum-mechanical sum rules employed in the derivation of Eqs. (52) and (54). Furthermore, the non-resonance case is considered and the transition probability is expanded up to the first order in the nuclear-displacement coordinate. From the results obtained herein, we conclude that:

(a) Two pure electronic states, i.e., the intermediate state k and the vibronically coupled state p , contribute to the intensity of the symmetry forbidden $g \rightarrow f$ two-photon transition.

(b) When the dipole transition between the ground state and the intermediate state is allowed (i.e., $M_{gk}^0 \neq 0$ and $M_{kf}^0 = 0$) it is required that either M_{kp}^0 and $(W_{fp})_a$ are nonvanishing for some values for p and a , or alternatively, that a pair of the matrix elements M_{fp}^0 and $(W_{kp})_a$ are nonvanishing. On the other hand, when the dipole transition between the intermediate and final electronic states is symmetry allowed (i.e., $M_{kf}^0 \neq 0$ and $M_{gk}^0 = 0$) it is required that at least one pair of the matrix elements M_{gp}^0 and $(W_{kp})_a$ or the pair M_{kp}^0 and $(W_{gp})_a$ should be nonvanishing.

(c) Mixing of two electronic states, say t and u , under a vibrational perturbation is determined by the integrals $(W_{tu})_a$. It is required that the states t and u should differ in the occupancy of a single MO and that

the direct product of the symmetry species Γ_t and Γ_u corresponding to the electronic states and the symmetry species Γ_a corresponding to the a th normal mode, must contain the totally symmetric representation. Thus Γ_a must correspond to at least one of the species contained in the direct product $\Gamma_t \times \Gamma_u$.

(d) The vibrational structure is determined by the vibrational integrals $\langle gi | q_a | fj \rangle$ characterized by the normal modes a for which the electronic terms δ_a do not vanish. Thus, it is expected that for the case of symmetry-forbidden two-photon transitions, the 0-0 line will be missing and vibrational progressions based on a non-totally-symmetric vibration will be observed.

(e) The total intensity of a symmetry-forbidden two-photon transition is expected to exhibit a temperature dependence determined by the factor $\coth(\hbar\omega_a/2kT)$, which is of the same form as for single-photon symmetry-forbidden transitions.

IV. CALCULATION OF ABSORPTION CROSS SECTIONS IN BENZENE

A. Evaluation of Electronic Integrals

In order to evaluate the electronic integrals appearing in the expression defining the mixing coefficient λ_{tu} , it is first necessary to obtain the one-electron transition density ρ_{tu} . The molecular orbitals that are used to define the lowest excited states of benzene are given in the LCAO approximation²⁰:

$$\begin{aligned}\theta_1 &= 0.3238(\omega_1 + \omega_2 + \omega_3 + \omega_4 + \omega_5 + \omega_6), \\ \theta_2 &= 0.2637(2\omega_1 + \omega_2 - \omega_3 - 2\omega_4 - \omega_5 - \omega_6), \\ \theta_3 &= 0.4567(\omega_2 + \omega_3 - \omega_5 - \omega_6), \\ \theta_4 &= 0.5855(-\omega_2 + \omega_3 - \omega_5 + \omega_6), \\ \theta_5 &= 0.3381(2\omega_1 - \omega_2 - \omega_3 + 2\omega_4 - \omega_5 - \omega_6), \\ \theta_6 &= 0.5485(\omega_1 - \omega_2 + \omega_3 - \omega_4 + \omega_5 - \omega_6),\end{aligned}\quad (55)$$

where $\omega_1 \cdots \omega_6$ are $2p_z$ atomic orbitals for carbon atoms, the MO's are normalized to include overlap. The ground state of benzene is written as a determinantal wavefunction:

$$\Theta_0 = (6t)^{-1/2} | \theta_1 \bar{\theta}_1 \theta_2 \bar{\theta}_2 \theta_3 \bar{\theta}_3 |. \quad (56)$$

The excited-state wavefunctions are written as a sum of the configurations χ_k^i corresponding to the one-electron excitations $\theta_k \rightarrow \theta_i$. The appropriate functions, symmetries, and observed and calculated energies are presented in Table I.

By carrying out the integration indicated in Eq. (34), and then expanding over atomic orbitals, the transition density can be represented by a set of point charges $-e\omega_\sigma^2$ located on atoms σ , and point charges $-eS_{\sigma,\sigma+1}$ at a point midway between atom σ and atom $\sigma+1$.²⁹ $S_{\sigma,\sigma+1}$ is the overlap integral between the two

TABLE I. Excited-state benzene wavefunctions.

Function	Symmetry	Energy (eV) (exptl)	I ^b	II ^a
$\theta_a = 2^{-1}(\chi_3^5 - \chi_2^4)$	B_{2u}	5.9	5.21	3.68
$\theta_b = 2^{-1}(\chi_3^4 + \chi_2^5)$	B_{1u}		6.32	5.76
$\theta_\gamma = 2^{-1}(\chi_1^5 - \chi_2^6)$	$E_{2g,a}$	6.2 ^a	8.30	5.93
$\theta_{\gamma'} = 2^{-1}(\chi_1^4 - \chi_3^6)$	$E_{2g,b}$			
$\theta_\delta = 2^{-1}(\chi_1^5 + \chi_2^6)$	$E_{2g,a}$		9 ^b	
$\theta_{\delta'} = 2^{-1}(\chi_1^4 + \chi_3^6)$	$E_{2g,b}$			
$\theta_\beta = 2^{-1}(\chi_3^5 + \chi_2^4)$	$E_{1u,a}$	7.0	7.48	6.98
$\theta_{\beta'} = 2^{-1}(\chi_3^4 - \chi_2^5)$	$E_{1u,b}$			

^a As yet undetermined.^b Pariser, Parr+CI, six excited configurations.²⁵^c Theoretical result of a CI calculation with six excited configurations.²⁶^d This is an approximate value, not calculated in Ref. 25.

adjacent atom orbitals. The integrals $(W_{ks})_a$ may then be evaluated empirically.²⁹ Liehr³¹ has shown how the corresponding integrals may be evaluated non-empirically. He defined the integrals $I_\sigma^f(s, k, a)$ related to the matrix element $(W_{ks})_a$ in the following way:

$$(W_{ks})_a = \sum_{\sigma} \sum_{f=1}^3 I_\sigma^f(s, k, a). \quad (57)$$

The superscript f denotes the Cartesian components of the radius vector \mathbf{r}_σ . Only in-plane components of the vibrations denoted $f=R$, U are considered in the calculation; R and U indicating radial and perpendicular displacements of the carbon atoms, respectively.

A complete calculation of forbidden intensities in benzene was presented by Albrecht,³⁰ who illustrated how the integrals $I_\sigma^f(s, k, a)$ may be used, and derived relationships between them so that only a minimum number of integrals need be calculated, the rest immediately obtainable from symmetry considerations. In our case, only I_1^R and I_2^U , corresponding to the radial and perpendicular contributions of Atoms 1 and 2 in the ring, are needed. We have adjusted the formalism of Murrell and Pople so that direct comparison of the semiempirical and nonempirical method of calculating the electronic integrals may be made. In Table II, we present the values of the integrals given by Albrecht for the different transition densities and the corresponding results derived from the Murrell-Pople method. Table III contains the calculated single-photon oscillator strengths for benzene, using both methods. In addition, we have reported results obtained by including ground-state mixing in the calculation. This seems to have a marked effect on the B_{2u} state oscillator strength. This is to be expected since the energy denominator $E_{B_{2g}} - E_{A_{1g}} = 6.2$ eV corresponds to about 34% of the energy denominator involved in mixing the B_{2u} state, i.e., $E_{B_{1u}} - E_{B_{2u}} = 2.1$ eV. The effect of ground-state mixing on other transitions is much smaller; in the two-photon case, the contribution

of ground-state mixing is not expected to be more than 10%. Both the empirical and nonempirical electronic integrals appearing in Table II were used for the calculations of the two-photon absorption cross sections.

The general expression for two-photon cross sections involving vibronically induced transitions requires the calculation of transition moments between excited states. These have been calculated with the MO's given above for benzene in the usual way,³² applying the dipole approximation.

B. Angular Dependence

The expression¹⁹ for the absorption cross sections involves the scalar products between the polarization vector of the light \mathbf{e}_λ and the polarization of the transitions \mathbf{r}_{oi} and \mathbf{r}_{ij} . The angular dependence must be included in the summation and its square, and then be summed over all possible molecular orientations to yield a mean two-photon capture cross section. When photons of different polarization and frequency are involved, the angular dependence of each summation must be evaluated separately because of the different energy denominators that appear. Evleth and Peticolas¹⁹ have derived the orientation factors when the two photons are taken to have the same polarizations. Considering the case when the two photons have different energies and polarizations, we present only the angular dependence of the various scalar products. Assume the z axis to be defined by the direction of polarization of one of the beams \mathbf{e}_z , the transition moments \mathbf{r}_{oi} and \mathbf{r}_{ij} are either parallel or perpendicular to each other as is the case in molecules of D_{6h} or D_{2h} symmetry. The second photon may have any polarization direction in space with respect to the first, but will define the yz

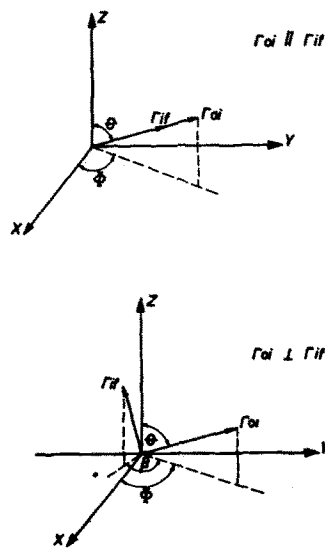


FIG. 1. Coordinate system for the calculation of the polarization dependence of the two-photon transition.

³² R. Daudel, R. Lefebvre, and C. Moser, *Quantum Chemistry* (Interscience Publishers, Inc., New York, 1959), pp. 216-220.

TABLE II. Electronic integrals.

Transition	δ_{ik}	Symmetry	Empirical		Nonempirical	
			I_1^R (eV/Å)	I_2^U	I_1^R (eV/Å)	I_2^U
0- B_{2u}	$\theta_a\theta_\beta$	e_{2g_a}	-1.94	1.18	-1.18	2.28
0- B_{1u}	$\theta_p\theta_\beta$	e_{2g_a}	2.36	5.97	1.10	3.17
0- E_{2g}	$\sqrt{2}\theta_p\theta_\beta$	e_{1u_a}	-1.43	3.65	-0.13	3.51
0- E_{2g}	$\sqrt{2}\theta_\beta\theta_\beta$	e_{1u_a}	400	3.00	1.70	1.22

plane; that is, its direction of polarization will be along the y axis when it is perpendicular to \mathbf{e}_z . In fact, we assume it to be either parallel or perpendicular to the first photon, all other possibilities being expressible in terms of these special cases. The usual polar angles θ and ϕ refer to the orientation of \mathbf{r}_{oi} . If \mathbf{r}_{if} is perpendicular to \mathbf{r}_{oi} , β is the angle between the molecular plane and the plane defined by \mathbf{r}_{oi} and the z axis (Fig. 1). The following scalar products arise:

$$\begin{aligned}(\mathbf{r}_{oi} \cdot \mathbf{e}_z) &= |\mathbf{r}_{oi}| \cos\theta, \\ (\mathbf{r}_{oi} \cdot \mathbf{e}_y) &= |\mathbf{r}_{oi}| \sin\theta \cos\phi.\end{aligned}\quad (58)$$

The same relationships hold for \mathbf{r}_{if} if it is parallel to \mathbf{r}_{oi} . If \mathbf{r}_{if} is perpendicular to \mathbf{r}_{oi} , we write

$$\begin{aligned}(\mathbf{r}_{if} \cdot \mathbf{e}_z) &= |\mathbf{r}_{if}| \sin\theta \cos\beta, \\ (\mathbf{r}_{if} \cdot \mathbf{e}_y) &= |\mathbf{r}_{if}| (\cos\theta \sin\phi + \sin\beta \sin\theta \cos\phi).\end{aligned}\quad (59)$$

The angular terms are integrated over the volume element $\sin\theta d\theta d\phi d\beta$ and divided by the appropriate normalization factor, $8\pi^2$.

If the second beam is at an angle α with respect to the first, then the angular dependence along the y and z axes are first calculated, the former then multiplied by $\sin^2\alpha$ and the latter by $\cos^2\alpha$. The squares arise because the entire summation over intermediate states is squared. Terms in $\sin\alpha \cos\alpha$ turn out to be zero.

C. Two-Photon Absorption in Benzene

The evaluation of two-photon cross sections in benzene can be accomplished with the use of Tables

TABLE III. Oscillator strengths.

	Murrel and Pople		Albrecht		Observed
	a	b	a	b	
fB_{2u}	0.005	0.009	0.006	0.011	0.0014
fB_{1u}	0.185	0.208	0.052	0.069	0.094
fE_{2g}	0.019	0.025	0.033	0.040	0.094
fE_{2g}	0.112	0.112	0.019	0.019	0.094

^a Reported in reference—Murrel and Pople values corrected for a slight error normalization in Whiffen's normal-coordinate analysis of benzene.²¹

^b Method "a" with ground-state mixing included in calculation.

I-IV and Eq. (19). [Note added in proof: The transition matrix elements presented herein were calculated from Eq. (14). The same conclusions concerning the relative magnitude of the two-photon absorption cross section are obtained by the application of Eq. (14a).] The summation is taken over all singlet excited states arising from $\pi \rightarrow \pi^*$ excitations, but intermediate states involving two forbidden transitions are considered. In Table IV, we list the pathways of two-photon absorption to the four lowest singlet excited states in benzene and the vibrations mixing the forbidden transitions involved.

The energies of the B_{2u} and E_{1u} states were taken from the experimental data as reported in Table I. The E_{2g}^γ state (as indicated in various theoretical calculations²²) is assumed to be the lower of the two E_{2g} states. The upper E_{2g}^δ state was located at 9 eV²²; the calculations are quite insensitive to its exact energy. The energies of the B_{1u} and E_{2g}^γ states were treated as parameters in the calculation; that is, one state is located at the experimental value of 6.2 eV, and its cross section evaluated for different energy values of the other. When the E_{2g}^γ is located at 6.2 eV, the B_{1u} state energy is varied in the range 6.9 to 7.5; when the B_{1u} state is located at 6.2 eV, the E_{2g}^γ state energy is varied in the range 6.9 to 7.9. This range of variation is indicated by theoretical calculations, though in no case does the B_{1u} state have a higher energy than the calculated E_{1u} state.

Laser energies of both 1.8 eV (which can be obtained from the ruby laser) and 3.6 eV (which can be obtained by second-harmonic generation) are used in the calculations. Absorption measurements can be, in principle, carried out with a second light source whose frequency matches the energy difference between the laser frequency and that of the final molecular state.⁷ Experiments can be performed in the range where the energy of the secondary source does not overlap the range of single-photon absorption, starting at about 4.4 eV. Thus, for the 1.8-eV laser beam, only regions corresponding to total energies of up to $4.4+1.8=6.2$ eV may be scanned. It will be possible to reach energies of up to 8.0 eV if the second-harmonic 3.6-eV laser beam is used.

Tables V and VI contain the calculated values of a parameter $\delta = \sigma(\omega)/F_\lambda$ used to characterize the cross

TABLE IV. Pathways of two-photon transitions.^a

Transition	Pathways	Mixing vibration
$A_{1g} \rightarrow B_{2u}$	$A_{1g} \rightarrow E_{1u}, E_{1u} \xrightarrow{*} B_{2u} + A_{1g} \xrightarrow{*} E_{2g}, E_{2g} \xrightarrow{t} B_{2u}$	e_{1u}
$A_{1g} \rightarrow B_{1u}$	$A_{1g} \rightarrow E_{1u}, E_{1u} \xrightarrow{*} B_{1u} + A_{1g} \xrightarrow{*} E_{2g}, E_{2g} \gamma \rightarrow B_{1u}$	e_{1u}
$A_{1g} \rightarrow E_{1u}$	$A_{1g} \xrightarrow{*} E_{2g}, E_{2g} \gamma \rightarrow E_{1u}$	e_{1u}
$A_{1g} \rightarrow E_{2g}$	$A_{1g} \rightarrow E_{1u}, E_{1u} \rightarrow E_{2g} \gamma + A_{1g} \xrightarrow{*} B_{1u}, B_{1u} \rightarrow E_{2g} \gamma$	e_{2g}

^a An asterisk indicates a symmetry-forbidden transition.TABLE V. Calculated two-photon absorption cross sections—benzene. [$g(\omega) = 10^{-14} \text{sec.}$]

Energies (eV)		Parallel beams				Perpendicular beams			
		$\delta \times 10^{50} (\text{cm}^4 \cdot \text{sec atom}^{-1} \cdot \text{photon}^{-1})$				$\delta \times 10^{50} (\text{cm}^4 \cdot \text{sec atom}^{-1} \cdot \text{photon}^{-1})$			
B_{1u}	E_{2g}	B_{2u}	B_{1u}	E_{1u}	E_{2g}	B_{2u}	B_{1u}	E_{1u}	E_{2g}
A. Nonempirical^a									
6.2	6.9	0.75	1.50			0.79	0.35		
6.2	7.1	0.94	0.04			0.10	0.01		
6.2	7.3	1.14	0.20			1.18	0.04		
6.2	7.5	1.30	0.71			1.34	0.20		
6.2	7.7	1.46	1.30			1.50	0.32		
6.2	7.9	1.62	1.85			1.62	0.47		
6.9	6.2	0.05			353	0.08			209
7.1	6.2	0.05			472	0.08			299
7.3	6.2	0.05			176	0.08			78
7.5	6.2	0.05			147	0.08			56
B. Semiempirical^a									
6.2	6.9	3.98	0.87			4.50	0.24		
6.2	7.1	5.48	0.03			5.64	0.01		
6.2	7.3	6.55	0.12			6.70	0.04		
6.2	7.5	7.53	0.43			7.69	0.12		
6.2	7.7	8.44	0.75			8.60	0.20		
6.2	7.9	9.23	1.06			9.39	0.28		
6.9	6.2	0.28			935				646
7.1	6.2	0.28			1360				966
7.3	6.2	0.28			313				181
7.5	6.2	0.28			212				105
C. Nonempirical^b									
6.2	6.9	0.87	0.79	3.31	3.82	0.99	0.20	2.48	2.25
6.2	7.1	1.10	0.02	3.12	5.52	1.22	0.01	2.33	3.55
6.2	7.3	1.34	0.32	2.96	17.6	1.46	0.08	2.31	7.65
6.2	7.5	1.58	0.83	2.80	40.2	1.70	0.20	2.13	14.9
6.2	7.7	1.77	1.38	2.68	75.0	1.89	0.35	2.01	25.6
6.2	7.9	1.93	1.85	2.60	123	2.05	0.47	1.93	41.0
6.9	6.2	0.04	20.7	4.2	227	0.16	5.2	3.16	129
7.1	6.2	0.04	14.4	4.2	312	0.16	3.59	3.16	190
7.3	6.2	0.04	11.7	4.2	170	0.16	2.92	3.16	48.5
7.5	6.2	0.04	10.6	4.2	101	0.16	2.64	3.16	34.5
D. Semiempirical^b									
6.2	6.9	4.73	0.43	1.93	10.4	5.72	0.10	1.42	7.18
6.2	7.1	6.47	0.01	1.81	16.5	7.14	0.00	1.34	11.8
6.2	7.3	7.81	0.20	1.74	34.3	8.48	0.04	1.30	20.2
6.2	7.5	9.03	0.47	1.66	64.7	9.70	0.11	1.22	33.1
6.2	7.7	10.1	0.79	1.58	109	10.8	0.20	1.18	51.3
6.2	7.9	11.2	1.06	1.50	171	11.8	0.28	1.14	76.5
6.9	6.2	0.24	12.1	2.44	591	0.91	3.00	1.85	401
7.1	6.2	0.24	8.40	2.44	880	0.91	2.09	1.85	618
7.3	6.2	0.24	6.78	2.44	211	0.91	1.70	1.85	116
7.5	6.2	0.24	6.15	2.44	145	0.91	1.54	1.85	67.0

^a $\hbar\nu_{\text{laser}} = 1.8 \text{ eV.}$ ^b $\hbar\nu_{\text{laser}} = 3.6 \text{ eV.}$

sections of a two-photon absorption. Both semiempirical and nonempirical results are tabulated. In each case, results are reported for both mutually parallel ($\mathbf{e}_\lambda \parallel \mathbf{e}_\mu$) and perpendicular ($\mathbf{e}_\lambda \perp \mathbf{e}_\mu$) polarization of the two beams. Blanks in Table V correspond to energies where single-photon absorption of the secondary beam is expected.

The B_{2u} , B_{1u} , and E_{1u} two-photon transitions all proceed via forbidden pathways, each mixed by vibrations of e_{1u} symmetry. Their vibrational structure is determined by the relative displacements of each of the e_{1u} vibrations, and by the electronic integrals $I_1^R(s, k, e_{1u})$ and $I_2^U(s, k, e_{1u})$. The vibrational structures of the B_{2u} , B_{1u} , and E_{1u} bands are independent of any energy parameters in the approximation we have been using, i.e., no terms of higher order than q_a appear in the calculation of the cross sections. Table VII contains relative contributions of each vibration to the total intensity of each band mixed by e_{1u} vibrations.

The vibrational structure of the E_{2g} band should be strongly dependent on energy parameters. The two-photon transition involves both forbidden and allowed pathways; the allowed going via the E_{1u} intermediate, and the forbidden via the B_{1u} vibronically coupled with the E_{1u} by e_{2g} vibrations. Since the intensity of the allowed transition is generally an order of magnitude greater than that of the vibronically induced transition, the e_{2g} vibrations will probably not be observed. If, however, B_{1u} state is close to the E_{1u} state in energy, vibrational structure should appear, corresponding to a large increase of the contribution of the forbidden pathway. Table VII contains the relative contributions of the e_{2g} vibrations to the intensity of the vibronically induced E_{2g} transition.

V. DISCUSSION

The theoretical results obtained herein strongly indicate that a good deal of information may be obtained from two-photon absorption experiments in benzene and other aromatic molecules. The question of choosing between the $(\mathbf{P} \cdot \mathbf{A})$ and A^2 terms in the interaction Hamiltonian presents no problem except in extreme

TABLE VII. Relative vibrational contributions of the e_{2g} vibration for two-photon transitions in benzene.

Transition	Nonempirical				Semiempirical			
	e_{2g} Vibrations in cm^{-1}				e_{2g} Vibrations in cm^{-1}			
	606	1177	1595	3047	606	1177	1595	3047
$0-E_{2g}$	0.16	0.06	0.77	0.01	0.12	0.06	0.81	0.01

cases. The A^2 term was shown to contribute about 0.1% of the intensity in allowed two-photon transitions. Most of the forbidden transitions tabulated in Tables V and VI have cross sections of 1%–10% of the allowed transition. All the cross sections vary considerably with the energy assignments of the various states. The mean value of δ for the E_{2g} state is about $5 \times 10^{-49} \text{ cm}^4 \text{ sec}^{-1}$. Thus, the A^2 term might be expected to make contributions to transitions with δ values of about $10^{-58} \text{ cm}^4 \cdot \text{sec}$. Extremely weak forbidden transitions may probably include an intensity contribution of the order of 10% from the A^2 term. The A^2 term will not contribute if the two beams are mutually perpendicular, a fact which enables its role to be effectively determined. Our results indicate a strong possibility of deciding between the B_{1u} and the E_{2g} assignments of the 2000-Å one-photon absorption band of benzene. The major conclusions may be drawn from intensity comparisons, though vibrational structure, temperature dependence, and, to an extent, polarization dependence, may also provide useful information.

Tables V and VI provide a reasonable picture of the general band structure of two-photon absorption in benzene. The essential differences between the semiempirical and nonempirical methods involve absolute values, and not the relative intensities in which we are interested. As mentioned above, two possible energy assignments are predicted by theory.²⁵ In the first, the B_{1u} state is located at 6.2 eV, the E_{2g} being somewhere above the E_{1u} , between 7.0 and 8.0 eV. In the other, the E_{2g} state is at 6.2 eV, the B_{1u} state being located near the E_{1u} state, somewhere around 7.0 eV. The essential criterion in determining between the two possibilities is that Case (1) and Case (2) give decidedly different pictures of the predicted spectrum.

A. Intensity Comparisons

1. Case (1)

For the 3.6-eV beam, weak lines of approximately equal intensity should appear at 4.9, 6.2, and 7.0 eV corresponding to the B_{2u} , B_{1u} , and E_{1u} transitions. The B_{1u} band appears to be slightly weaker than the other two, particularly when the E_{2g} is assumed to be at

TABLE VI. Relative vibrational contributions of the e_{1u} vibration for two-photon transitions in benzene.

Transition	Nonempirical			Semiempirical		
	e_{1u} Vibrations in cm^{-1}			e_{1u} Vibrations in cm^{-1}		
	3078	1480	1035	3078	1480	1035
$0-B_{2u}$	0.02	0.42	0.56	0.02	0.42	0.56
$0-B_{1u}$	0.00	0.35	0.65	0.02	0.78	0.20
$0-E_{1u}$	0.00	0.35	0.65	0.02	0.78	0.20

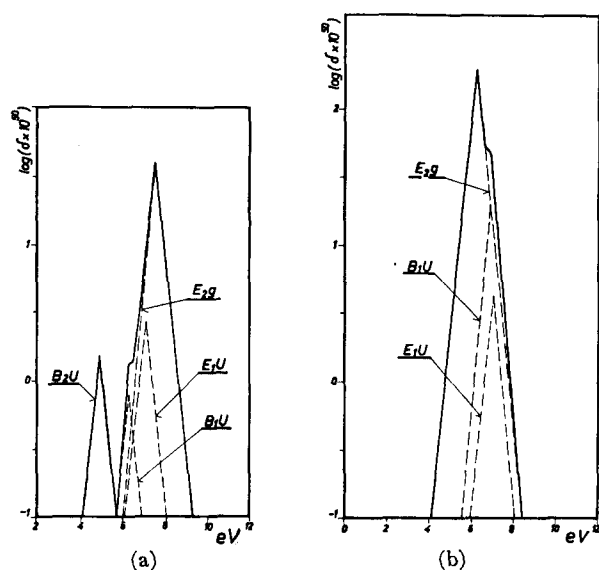


FIG. 2. Theoretically predicted two photon absorption spectra of benzene for the absorption of one photon $h\nu_\lambda = 3.6$ eV and a second photon $h\nu_\mu$. The two-photon energy is $E = h\nu_\lambda + h\nu_\mu$. (a) Case 1: B_{1u} state located at 6.2 eV. E_{2g} state located at 7.5 eV. (b) Case 2: E_{2g} state located at 6.2 eV. B_{1u} state located at 6.9 eV.

about 7.0 eV, near the E_{1u} state. The cross sections are otherwise essentially insensitive to the exact location of the E_{2g} state. There should also appear a strong band at above 7.0 eV corresponding to the E_{2g} absorption. The 1.8-eV beam only allows comparison between the B_{2u} and B_{1u} bands, the picture being essentially the same as before.

2. Case (2)

The B_{2u} band at 4.9 eV should be particularly weak. The E_{2g} absorption at 6.2 eV will be quite intense, at least a factor of 10 greater than the E_{1u} absorption at 7.0 eV. The picture is essentially the same when the 1.8-eV laser is used, though the E_{2g} should be even more intense, the E_{1u} state will, of course, not be observed.

The intensity of the B_{1u} absorption becomes quite small when the E_{2g} state is located near but above the E_{1u} state. This is a result of cancellation of the different terms contributing to the intensity, arising from energy denominators with opposite signs, but has no other apparent significance. Figure 2 contains the predicted two-photon absorption intensities for benzene for Cases (1) and (2) with the theoretically calculated excited-state energies taken from Table I. The laser beam is taken as 3.6 eV so that the entire spectrum may be scanned. The spectrum was calculated by assuming triangular absorption bands characterized by half-widths of 0.4 eV. The resultant spectrum obtained by summing the contribution of each state contains two peaks for Case (1) and one peak for Case (2). In each case, the strong E_{2g} absorption tends to mask both the

E_{1u} and B_{1u} bands. In Case (1) a shoulder appears on the low-energy side of the band, and in Case (2), on the high-energy side. The B_{2u} intensity is small in both cases, but negligible in Case (2). The following discussion on vibrational structure applies for individual bands which might be detected under conditions of relatively high resolution.

B. Vibrational Structure

Two-photon absorption bands resulting from vibronically induced mechanisms should exhibit vibrational states corresponding to the vibrations causing the mixing. If only one electronic state acts as an intermediate, the vibrational structure should be determined by the vibronic structure of the single-photon transitions to and from that state. If, further, the forbidden transition originates from the ground state, or is mixed by the same electronic integrals as some symmetry-forbidden one-photon transition, then its vibration structure will be known from the observed electronic spectra of benzene. These criteria are fulfilled for all the transitions considered in this work. Both pathways of the B_{2u} transition are mixed by the e_{1u} vibrations and involve the electronic integrals of the single-photon $A_{1g} \rightarrow E_{2g}$ transition. The B_{1u} and E_{1u} two-photon transition are both mixed by e_{1u} vibrations, and the $A_{1g} \rightarrow E_{2g}$ electronic integrals. The forbidden pathway of the E_{2g} two-photon transition is mixed up by e_{2g} vibrations and the $A_{1g} \rightarrow B_{1u}$ electronic integrals. In this case, the vibrational structure will probably be obscure because the forbidden pathway will, in general, contribute only a small fraction of the total intensity. The vibrational structure of each two-photon absorption band can be correlated with a given one-photon band with the aid of Table IV. Thus, for example, the two-photon B_{2u} transition has the same vibrational structure as the one-photon E_{2g} transition. This is only true because the forbidden $E_{1u} \rightarrow B_{2u}$ transition contains the same vibrational contributions as the $A_{1g} \rightarrow E_{2g}$ transition originating from the ground state. The same behavior holds true for the B_{1u} transition as well, but should not be taken as a general rule.

Case (1) and Case (2) may now be discussed in terms of vibrational structure.

For Case (1) the B_{1u} band at 6.2 eV should have the same structure as the E_{1u} band at 7.0 eV. This should differ from the one-photon B_{1u} envelope at 6.2 eV.

For Case (2) the E_{1u} band should have the same vibrational structure as the one-photon E_{2g} transition at 6.2 eV. The two-photon transition to the E_{2g} state should exhibit vibrational structure only if the forbidden pathway via the B_{1u} makes a sizable contribution to the total intensity. This will be the case if the B_{1u} is very close to the E_{1u} . Otherwise, the E_{2g} should have no structure resulting from vibronically mixed transitions.

C. Temperature Dependence

The information obtainable from temperature dependence is essentially the same as that from the vibrational structure. The E_{2g} band should exhibit little or no temperature dependence, depending on the relative contribution of the symmetry-forbidden pathway. The B_{1u} state should exhibit the same temperature dependence as the E_{1u} state.

D. Polarization Dependence

The polarization dependence is tabulated in terms of two extreme cases, mutually parallel or perpendicular electric-field vectors of the incident beams. The ratio $\delta_{||}/\delta_{\perp}$ for the B_{2u} , B_{1u} , and E_{1u} transitions is approximately 1:1, 4:1, and 4:3, respectively, and all are energy independent. The corresponding value is not constant for the E_{2g} transition since the allowed and forbidden pathways have different angular dependence. The ratio is seen from the table to vary from about 4:1 to 2:1 depending on the energy-level assignments. When the B_{1u} is close to the E_{1u} , the forbidden pathway makes a sizeable contribution and its angular dependence must also be considered. Unfortunately, the changes in intensity do not seem to be enough to enable definite conclusions to be drawn.

The approximations involved in the present theoretical treatment should be now considered. As mentioned above, we have not considered pathways involving two forbidden transitions. A rough analysis of these mechanisms showed that their contribution is negligibly small, and in no case will be greater than a few percent. In addition, we have neglected Rydberg states involved in mixing since their transition moments

are quite small.³³ The analysis presented above indicates that definite assignments may be made for two-photon absorption in benzene. In particular, the assignment of the electronic state of benzene located in the 2000-Å region should be possible on the basis of experimental results. Our calculations indicate that vibronic coupling should be considered as the main explanation of the presence of symmetry forbidden two photon absorption bands.

Some implications of our data for other aromatic molecules are of interest. Two-photon excitation of anthracene may be understood on the basis of vibronic coupling. Instead of assuming the presence of a final A_g or B_g state that satisfies the symmetry requirements for two-photon absorption, it is possible to postulate a direct $A_{1g} \rightarrow B_{2u}$ symmetry-forbidden absorption process. The experimental value for δ reported for anthracene by Hall *et al.*⁶ is 3×10^{-51} cm⁴·sec which is of the order of magnitude of the largest value of a forbidden-transition cross section we calculate for benzene. Assuming the vibronic-coupling integrals to be about the same for both molecules, this result is reasonable. A two-photon transition to the first singlet B_{2u} state of anthracene may proceed via the intermediate state B_{3u} with the $B_{3u} \rightarrow B_{2u}$ transition being vibronically induced. There are other possible pathways but the large oscillator strength of the B_{3u} transition ($f \approx 2.3$) indicate its contribution to be significant. Comparing Hall's⁶ result with the data we present in Tables V and VI, and noting that anthracene should have larger cross sections than benzene, we may reasonably assume that a full theoretical treatment of anthracene will yield suitable agreement with experiment.

³³ P. G. Wilkinson, Can. J. Phys. **34**, 596 (1956).